Supplementary Information

Electrical pumping and tuning of exciton-polaritons in carbon nanotube microcavities

Arko Graf[1,2†], Martin Held[1†], Yuriy Zakharko[1], Laura Tropf[2], Malte C. Gather[2*], and Jana Zaumseil[1*]

[1] *Institute for Physical Chemistry, Universität Heidelberg, D-69120 Heidelberg, Germany*

[2] *Organic Semiconductor Centre, SUPA, School of Physics and Astronomy, University of St Andrews, St Andrews KY16 9SS, United Kingdom*

[†]These authors contributed equally to this work.

* E-mail: mcg6@st-andrews.ac.uk, zaumseil@uni-heidelberg.de

SECTION 1 - Additional experimental data

Table S1 | Cavity detuning versus spacer thickness. Different spacer layer thicknesses used in this work and the corresponding cavity detuning with respect to the S_1 exciton of (6,5) SWCNTs.

	Layer thickness (nm)		Cavity detuning
	AlO_x spacer	**SWCNT**	**(meV)**
Reference	155	33	No
Cavity	155	33	−62
	130	19	+95
	170	19	−61
	190	19	−63
	220	19	−112
	250	19	−262
	310	19	−428

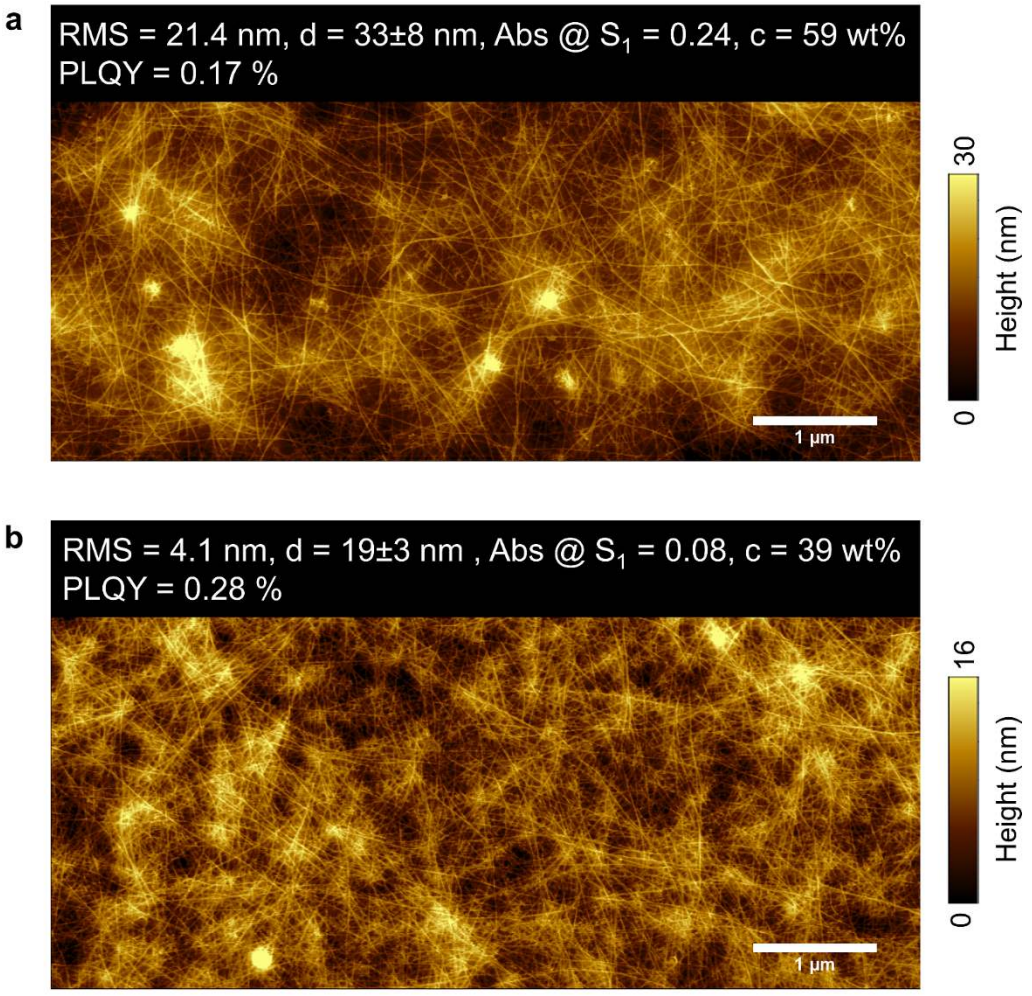

Figure S1 | Single-walled carbon nanotube networks used in LEFETs. a, **b**, Surface topography (tapping mode atomic force microscopy, Dimension Icon Atomic Force Microscope) of the two different SWCNT films used in this work. Surface roughness (root mean squared roughness, rms), thickness, absorption at S_1 transition (ABS @ S_1), SWCNT concentration in weight percent (wt%) and PL quantum yield (PLQY) are given at the top of each micrograph. Scale bar, 1 µm.

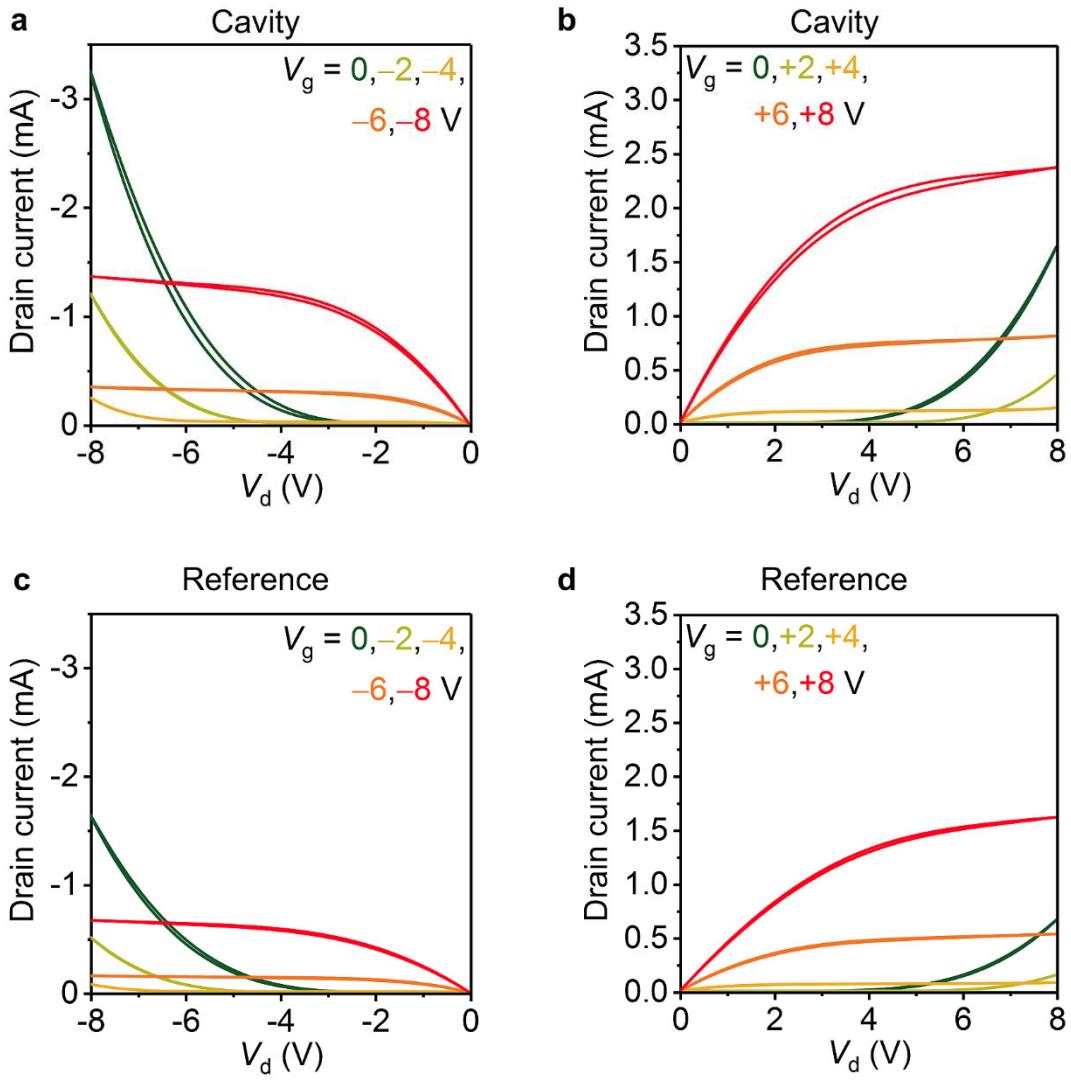

Figure S2 | Output characteristics for LEFETs. a, **b**, Cavity-embedded LEFET in strong coupling regime. **c**, **d**, Reference LEFET without bottom mirror. The output characteristics for low drain voltages are consistent with Ohmic contacts, corroborating low barriers for charge injection into the SWCNT layer.

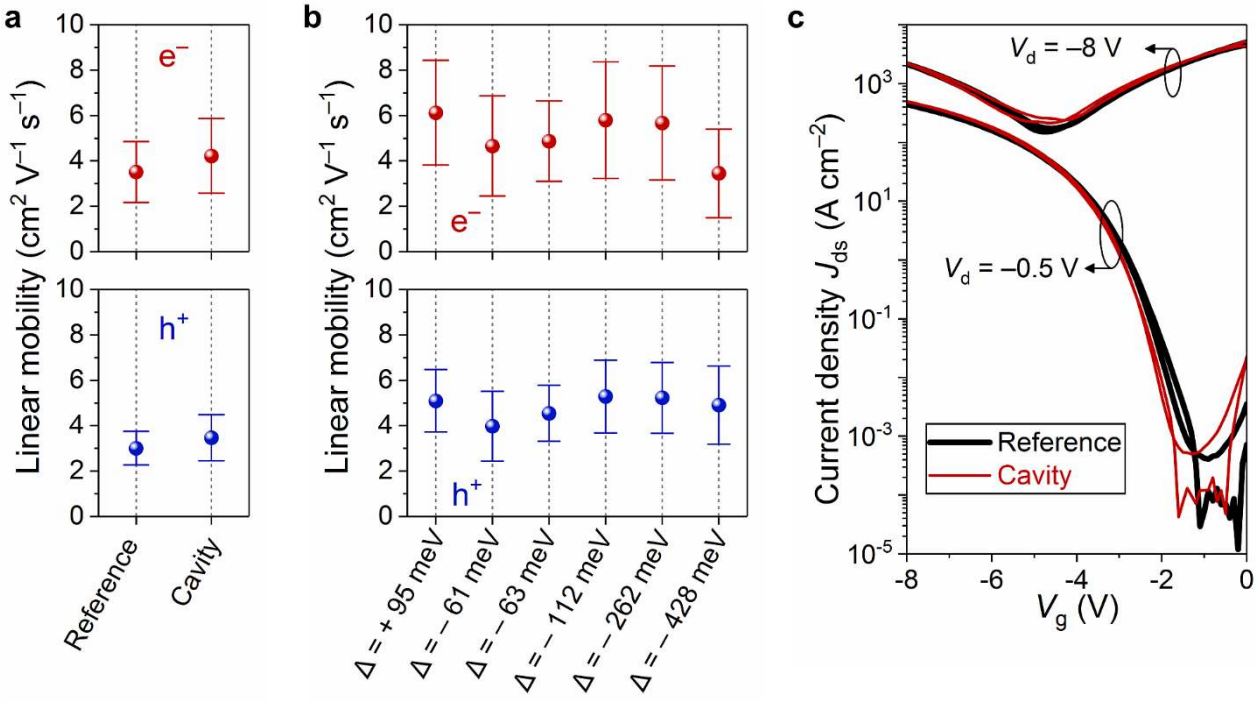

Figure S3 | Electrical performance of SWCNT-based LEFETs. a, Linear field-effect mobilities (electrons, holes) of LEFETs with a 33 nm thick SWCNT layer (see Figure S1a), with and without cavity. **b**, Linear field-effect mobilities versus cavity detuning for transistors with a smooth 19 nm thick SWCNT layer (see Figure S1b). **c**, Transfer characteristics of a reference LEFET (black) compared with a cavity-embedded LEFET (red). The absence of current hysteresis, small on-voltages of +0.3 V and −1.4 V for electrons and holes, respectively, confirm the high purity of the SWCNTs and the low defect-density of the dielectric. On-voltages are determined by the current onset at small drain bias (V_d = ±0.5 V). Linear charge carrier mobilities were calculated from the transfer characteristics at a drain voltage of V_d = ±0.5 V assuming the gradual channel approximation for field-effect transistors and using the measured areal capacitance of C = 100-150 nF cm^{-2}. No significant effect of the cavity and the strong coupling regime on the charge carrier mobility was observed.

(Note, these LEFETs were not optimized for fast switching; their geometry, gate capacitance and transconductance should lead to moderate cut-off frequencies of about 10 kHz.)

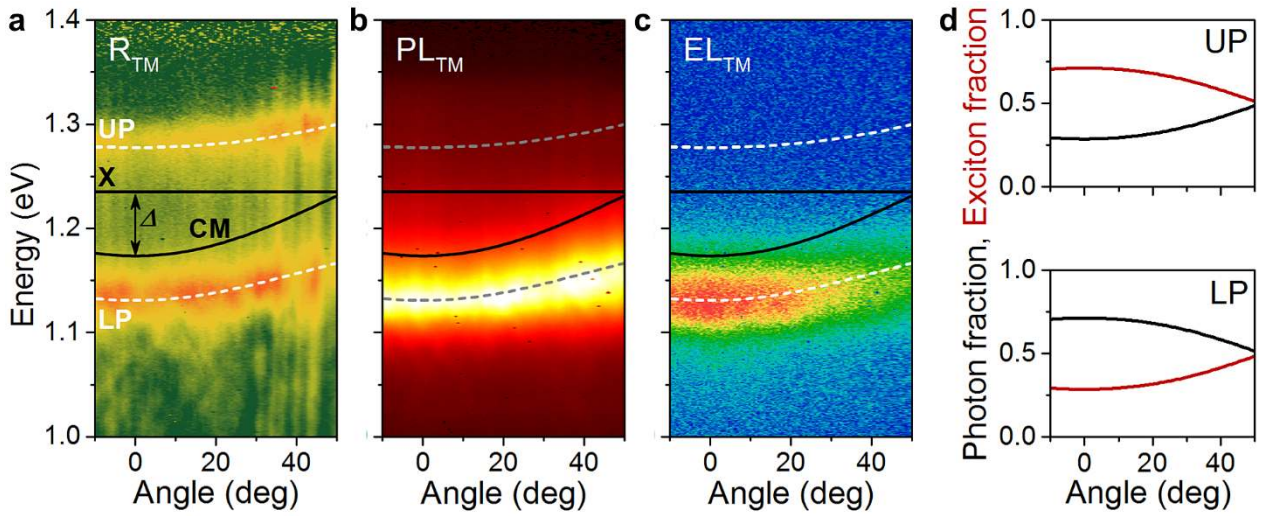

Figure S4 | Exciton-polaritons in cavity-embedded LEFETs (TM polarization). a, Angular reflectivity of the channel area in a cavity-embedded LEFET (channel length, $L = 5$ μm) with a dense (6,5) SWCNT layer. The dispersionless black solid line indicates the exciton (X) and the parabolic black line the cavity mode (CM). Strong exciton-photon coupling leads to the formation of a UP and LP mode (white dashed lines). These modes are fitted with the coupled oscillator model revealing a Rabi splitting ($\hbar\Omega$) of 133 meV with a cavity detuning (Δ) of −63 meV. **b**, Angle and spectrally resolved photoluminescence under optical excitation (640-nm cw-laser). **c**, Angle and spectrally resolved EL observed from the center of the channel at a current density of 600 A cm^{-2} ($V_d = -10$ V and $V_g = -5.1$ V). **d**, Angle-dependent photon and exciton fraction of the UP (top) and LP (bottom) as calculated by the coupled oscillator model.

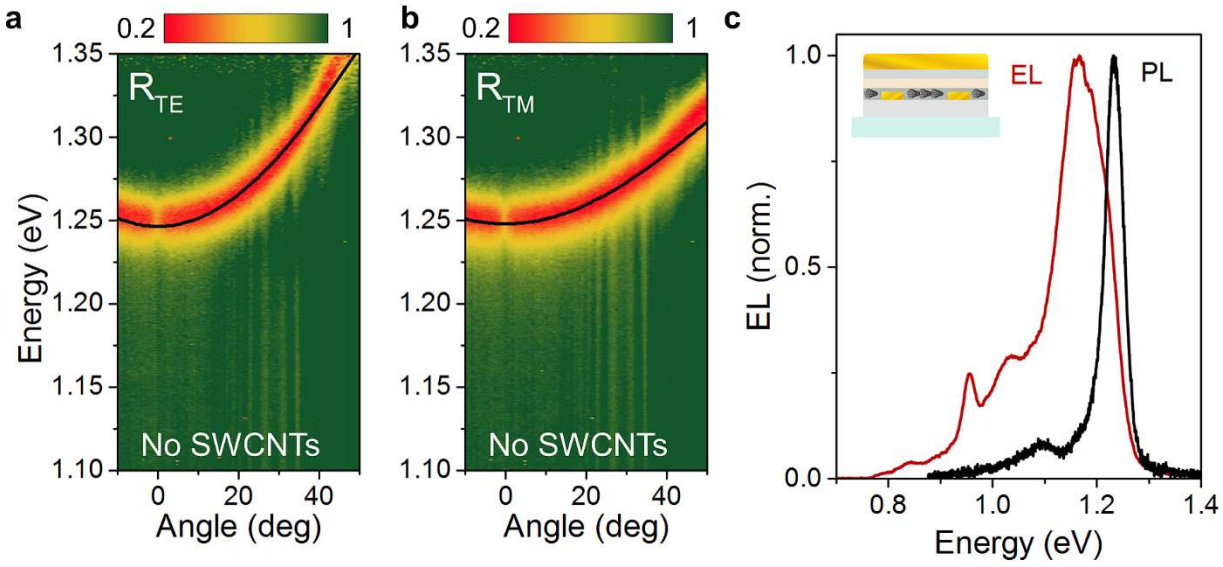

Figure S5 | Reference measurements for a cavity without SWCNTs. a,**b**, Data for TE and TM polarization. Fits to the parabolic cavity modes yield a cavity mode energy of E_0 = 1.248 eV and effective refractive indices of $n_{\text{eff}}^{\text{TE}}$ = 1.96 and $n_{\text{eff}}^{\text{TM}}$ = 2.53. The cavity has a HWHM of 22 meV, which corresponds to a quality factor (Q) of ~ 28. **c**, PL spectrum (black line) of a rough SWCNT layer (59 wt%) on glass under 575-nm laser excitation. The EL spectrum (red line) of a reference LEFET without a bottom mirror shows significant trion emission and energy transfer toward smaller bandgap SWCNT impurities.

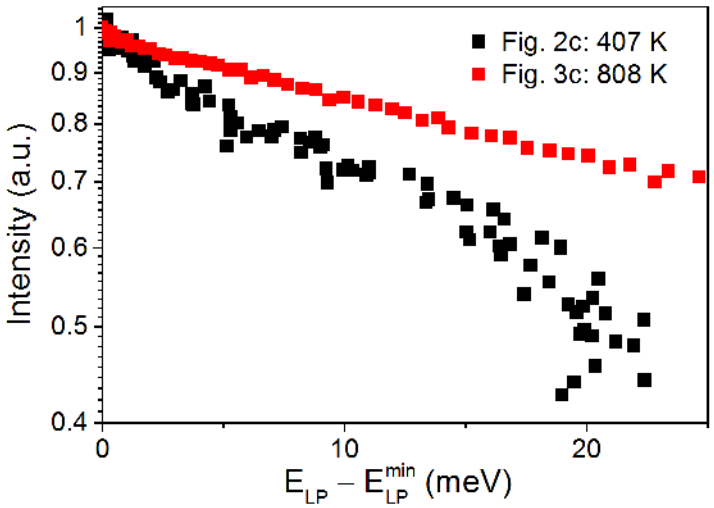

Figure S6 | LP occupancy of electrically pumped polaritons. The intensity distribution of the detected EL along the LP emission, divided by the photon fraction at a given energy, is proportional to the occupancy of the LP. The data were fitted with a Boltzmann distribution for the intensity, $\exp\left(\frac{\Delta E}{k_B T}\right)$ with ΔE being the energy difference and k_B the Boltzmann constant, resulting in the effective polariton temperature T, here 407 K for the data in Figure 2c (SWCNT thickness, 33 nm) and 808 K for the data in Figure 3c (SWCNT thickness, 19 nm). The Boltzmann-like distribution indicates the thermalization of polaritons.

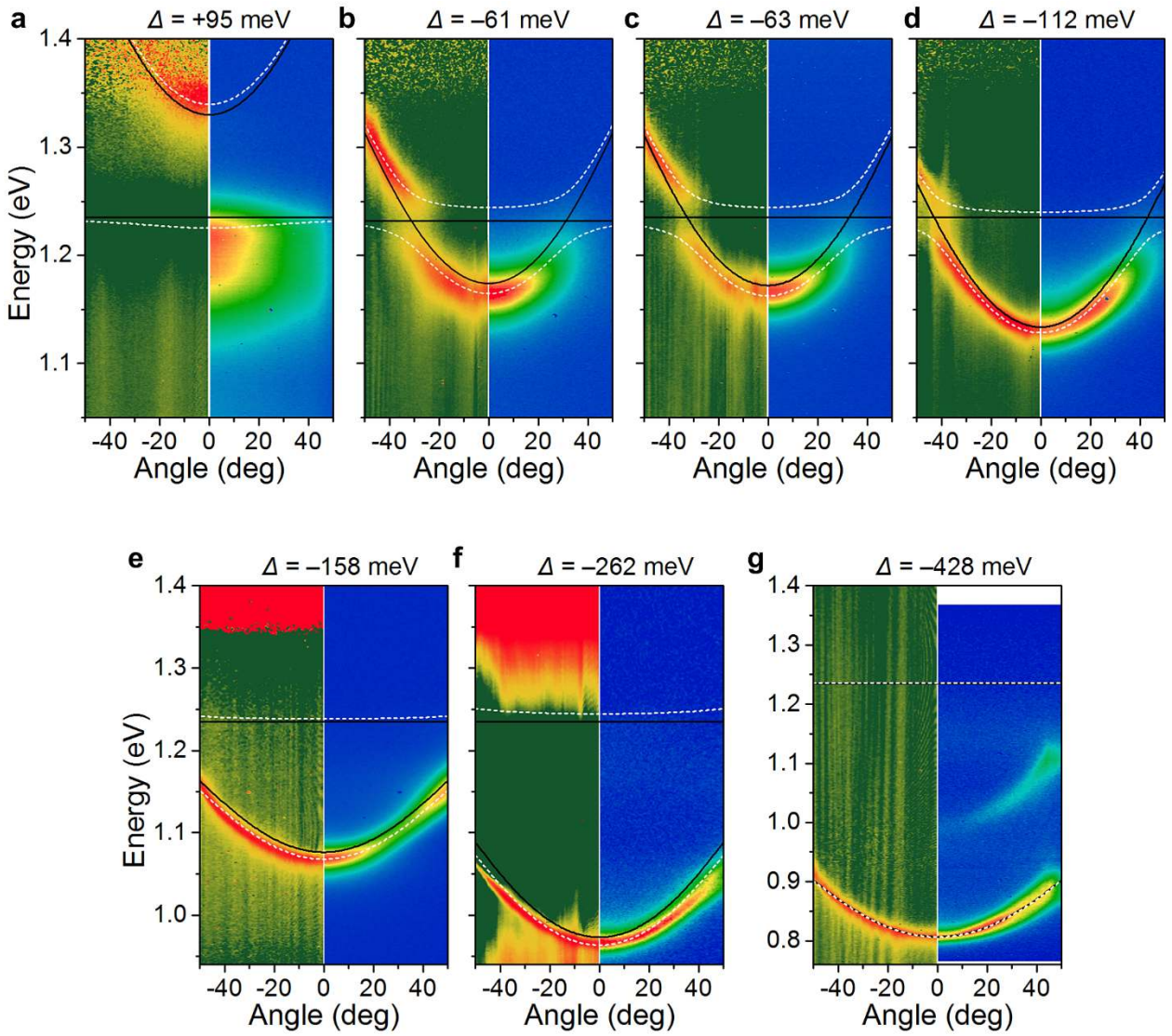

Figure S7 | Tuning exciton-polaritons in cavity-embedded LEFETs. Angular reflectivity of the channel area in cavity-embedded LEFETs (left) and EL (right) for different spacer layer thicknesses and thus detuning values Δ from +95 meV to −428 meV (see also Table S1) .

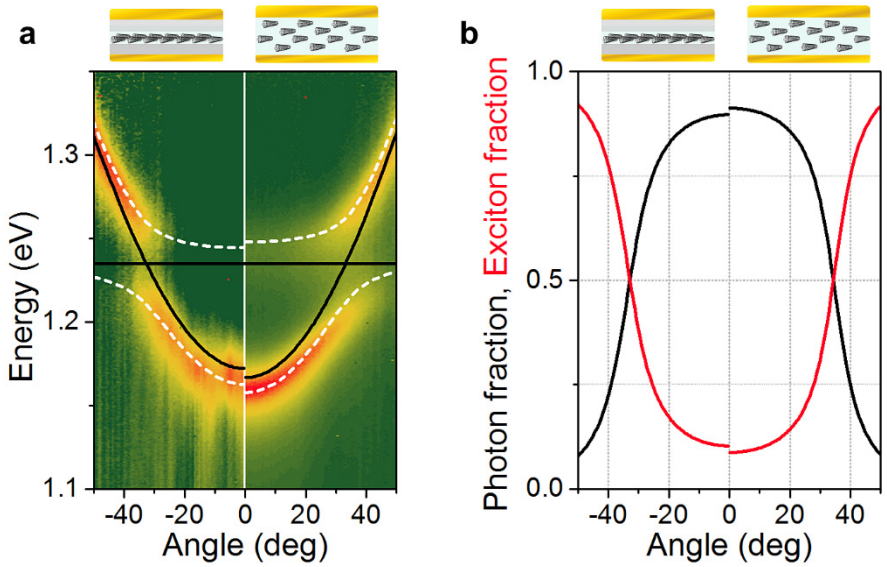

Figure S8 | Polariton relaxation for different SWCNT-densities. a, Angular reflectivity and **b**, fractions of the LP for the channel area in cavity-embedded LEFETs (left) and an optical microcavity as in Ref. 1 (right). The LEFET cavity has a 20 nm thick dense (39 wt%) SWCNT film sandwiched between spacer layers whereas the microcavity from Ref. 1 contains a homogeneous 250 nm thick polymer film with low SWCNT concentration (0.5 wt%). The polaritonic properties are almost identical for both devices (Rabi splitting 51 meV/54 meV and detuning −63 meV/−70 meV). However, at lower SWCNT density (right) a clear bottleneck effect is observed for polariton relaxation while the cavity with higher SWCNT density (left) shows more efficient/faster polariton relaxation as shown in Figure 4a.

1. Graf, A.; Tropf, L.; Zakharko, Y.; Zaumseil, J.; Gather, M. C., Near-infrared exciton-polaritons in strongly coupled single-walled carbon nanotube microcavities. *Nat. Comm.* **7**, 13078 (2016).

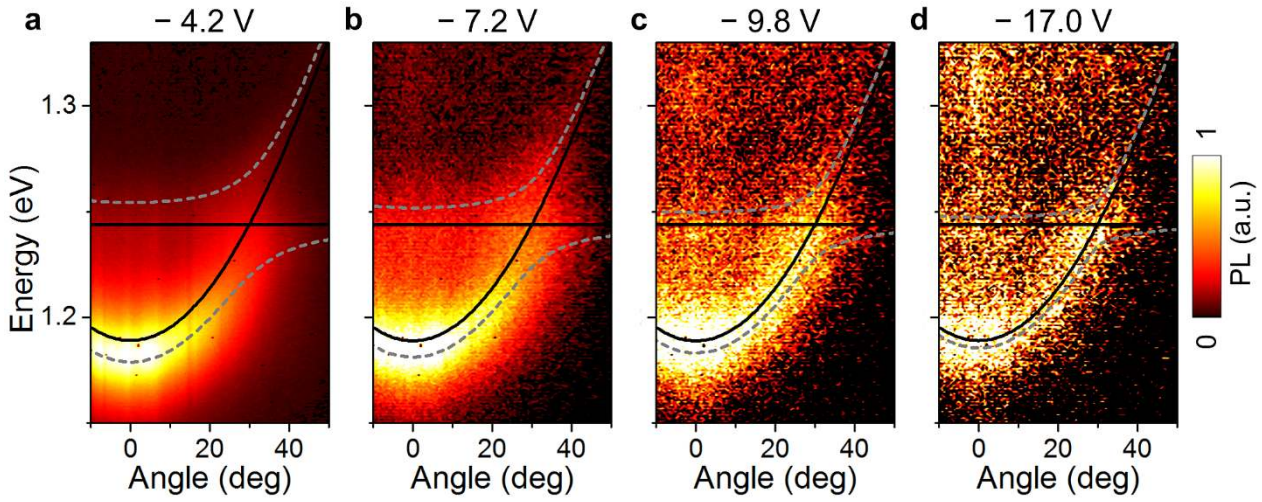

Figure S9 | Polariton emission upon charge accumulation. a to **e**, Angular PL for the four gate voltages corresponding to the reflectivity data shown in Figure 5b. In addition to reducing the oscillator strength and Rabi splitting (see Fig. 5b), the accumulation of holes leads to less efficient polariton relaxation, presumably due to the lower excitonic fraction of the LP at small angles.

SECTION 2 - Estimation of polariton density & ground state occupancy

Estimation of polariton density. We estimate that in our LEFET microcavity the exciton reservoir is pumped at a rate P of ~10^{27} cm^{-3} s^{-1} at the highest current density we use in this study (see Fig. 4b). In order to estimate the resulting polariton density in the LP, we use the rate equation approach. First, the exciton density in the reservoir n_{R} is given by

$$\frac{dn_{\mathrm{R}}}{dt} = \eta P - \frac{n_{\mathrm{R}}}{\tau_{\mathrm{therm}}} - \frac{n_{\mathrm{R}}}{\tau_{\mathrm{nr}}} . \qquad (1)$$

The non-radiative exciton lifetime τ_{nr} (15 ps) is calculated from the PLQY (0.3 %, see Fig. S1b) and the radiative lifetime (approx. 5 ns, see Ref. 1). Our cavity-embedded LEFETs do not show a relaxation bottleneck (see Fig. 4a), hence for a conservative estimate we can assume that the upper limit of the relaxation time into the LP (τ_{therm}) corresponds to the polariton lifetime (~20 fs, estimated from the FWHM). In addition, to account for the difference in EQE in the LEFET compared to the PLQY of the SWCNTs thin film, we introduce an internal conversion factor η (from the data in Fig. 3a we estimate η = 0.01).

The polariton density n_{LP} in the LP is described by

$$\frac{dn_{\mathrm{LP}}}{dt} = \frac{n_{\mathrm{R}}}{\tau_{\mathrm{therm}}} - \alpha\frac{n_{\mathrm{LP}}}{\tau_{\mathrm{cav}}} - \beta\frac{n_{\mathrm{LP}}}{\tau_{\mathrm{nr}}} . \qquad (2)$$

Here, the photon lifetime in the cavity τ_{cav} is determined by its quality factor Q. The mixed light-matter character of the LP is incorporated by using its photonic fraction α and excitonic fraction β. Additional losses from trion absorption by charged SWCNTs can be neglected because their oscillator strength is small.[2] This notion is supported by the small roll-off at high current densities in our LEFETs (see Fig. 3a). Assuming quasi steady-state conditions ($dn/dt \approx 0$), these equations allow us to estimate the polariton density in the LP (n_{LP}) as

$$n_{\mathrm{LP}} = \frac{\eta P}{\tau_{\mathrm{therm}}}\left(\frac{\alpha}{\tau_{\mathrm{cav}}} + \frac{\beta}{\tau_{\mathrm{nr}}}\right)^{-1}\left(\frac{1}{\tau_{\mathrm{therm}}} + \frac{1}{\tau_{\mathrm{nr}}}\right)^{-1} , \qquad (3)$$

which in our LEFET-cavity is ~$3.6\cdot10^{11}$ cm^{-3} for the electrical driving conditions used in this study.

Estimation of the ground state occupancy. For the determination of the mean ground state occupancy $\langle n_{k=0} \rangle$ we use the following estimate. In a single emission site within a diameter D of 1 μm (Fig. 1d) and a 5 nm depth w, we can estimate the number of polaritons to be

$$N_{LP} = n_{LP}\, w\, \pi D^2/4\ . \qquad (4)$$

Considering the occupancy at k = 0, we introduce a factor accounting for the fraction of polaritons emitting within ±1° (i.e., our detection resolution) compared to the detected ±50° by integration of the photon fraction corrected intensity along the LP. For the cavity shown in Figure 4b, this factor is found to be 0.03 and allows us to estimate the total number of polaritons within ±1° to be $0.03^2\, N_{LP}$. In order to estimate the ground state occupancy we reach in our devices, we then calculate the number of transverse states as:[3]

$$M = \frac{1}{2}\frac{\pi D^2/4}{4\pi^2}\pi(k_0 \Delta\theta)^2\ , \qquad (5)$$

with the wave number k_0 and $\Delta\theta$ = 0.0175 as the detection half angle. The mean ground state occupation is then given by:

$$\langle n_{k=0} \rangle = \frac{N_{LP}}{M}\ . \qquad (6)$$

For our metal-clad LEFET microcavity we reach an occupancy $\langle n_{k=0} \rangle$ of 0.004.

SECTION 3 - Toward polariton condensation and non-linear interactions

Considering the relevant loss and relaxation rates, we estimate the polariton density in the LP to be ~$3.6 \cdot 10^{11}$ cm^{-3} for our devices when operated at the current densities used in this work (see Section 2). By calculating the number of polaritons in a single emission site and the corresponding number of states in the ground state of the LP,[3] we find a mean polariton occupation of 0.004 per mode at k = 0 (see Section 2). Previously, a critical polariton density of ~10^{13} cm^{-3} was reported for polariton condensation in an optically pumped microcavity with a 120 nm thick layer of an organic emitter in the thermodynamic limit.[4] Given the thickness of the active layer in LEFETs (~5 nm) this value would translate into ~10^{14} cm^{-3} for our devices. In order to achieve these densities with cavity-embedded SWCNT LEFETs under electrical pumping and thus to obtain electrically driven polariton lasing, the polariton lifetime in our devices needs to be increased substantially. This can be accomplished by replacing the metal mirrors with highly reflective distributed Bragg reflector (DBR) mirrors. Integrating DBRs as bottom and top mirrors into an LEFET structure should be less challenging than for other device geometries because in an LEFET the cavity is spatially separated from the charge injecting electrodes and the charge transport layer and can thus be optimized independently. Using this concept the quality factor of our cavity could be increased to 1000, which would boost the polariton density in the LP to ~$1.3 \cdot 10^{13}$ cm^{-3}. In such a cavity the mean occupancy at k = 0 would rise to 0.15. Furthermore, by using aligned SWCNT films[5] and a double-gated architecture[6] the pumping rate could be readily increased by an order of magnitude, thus yielding the desired polariton density of 10^{14} cm^{-3} and reaching an occupancy larger than unity and the polariton lasing threshold.

Nonlinear polariton interactions based on the excitonic component of the polaritons rely on interacting excitons. Spatial overlap of the excitons is present if the Mott density, given by a_B^{-3}

where a_B is the Bohr radius, in our SWCNT films is reached. In our case (a_B for SWCNTs is ~10 nm, Ref. 7) this corresponds to 10^{18} cm^{-3}. Due to the high exciton diffusion length in SWCNTs, exciton interactions will be present at around 10^{15} cm^{-3}. In our devices we reach a polariton density of ~$3.6 \cdot 10^{11}$ cm^{-3}, which is well below the pure exciton Mott transition and possible exciton-exciton interaction based on exciton diffusion. This explains why we do not observe nonlinear interactions in our devices. As elaborated above, in an improved microcavity-LEFET polariton densities of 10^{14} cm^{-3} are readily achievable. In this regime, nonlinear interactions might be present for hybrid exciton-polaritons.

References

1. Miyauchi, Y., Hirori, H., Matsuda, K. & Kanemitsu, Y. Radiative lifetimes and coherence lengths of one-dimensional excitons in single-walled carbon nanotubes. *Phys. Rev. B* **80,** 81410 (2009).
2. Hartleb, H., Späth, F. & Hertel, T. Evidence for Strong Electronic Correlations in the Spectra of Gate-Doped Single-Wall Carbon Nanotubes. *ACS Nano* **9,** 10461–10470 (2015).
3. Deng, H., Weihs, G., Snoke, D., Bloch, J. & Yamamoto, Y. Polariton lasing vs. photon lasing in a semiconductor microcavity. *Proc. Natl. Acad. Sci.* **100,** 15318–15323 (2003).
4. Slootsky, M., Zhang, Y. & Forrest, S. R. Temperature dependence of polariton lasing in a crystalline anthracene microcavity. *Phys. Rev. B* **86,** 45312 (2012).
5. He, X. *et al.* Wafer-scale monodomain films of spontaneously aligned single-walled carbon nanotubes. *Nat. Nanotechnol.* **11,** 633–638 (2016).
6. Kim, B., Liang, K., Geier, M. L., Hersam, M. C. & Dodabalapur, A. Enhancement of minority carrier injection in ambipolar carbon nanotube transistors using double-gate structures. *Appl. Phys. Lett.* **109,** 23515 (2016).
7. Mann, C. & Hertel, T. 13 nm Exciton Size in (6,5) Single-Wall Carbon Nanotubes. *J. Phys. Chem. Lett.* **2016,** 2276–2280 (2016).